Biochemical and Physical Parameters of the Electrical Currents Measured with the ADP/ATP Carrier by Photolysis of Caged ADP and ATP†

Nikolay Broustovetsky,‡ Ernst Bamberg,§ Thiemo Gropp,§ and Martin Klingenberg*,‡

Institute of Physical Biochemistry, University of Munich, Schillerstrasse 44, D-80336 Munich, Germany, and Max-Planck-Institute for Biophysics, Kennedyallee 70, 60596 Frankfurt, Germany

Received June 30, 1997; Revised Manuscript Received August 28, 1997⊗

ABSTRACT: The transport by the mitochondrial ADP/ATP carrier (AAC) has been shown in a preliminary communication to produce electrical capacitive currents on photolysis of caged ATP or ADP with reconstituted AAC liposomes attached to black lipid membranes [Brustovetsky, N., Becker, A., Klingenberg, M., and Bamberg, E. (1996) *Proc. Natl. Acad. Sci. U.S.A. 93,* 664−668]. Here we study the relation of the currents to ADP/ATP fluxes, the interaction of caged ADP and ATP with AAC and other basic facets of this method. Caged ADP and ATP are not transported by the AAC, as shown in mitochondria. Flux measurements with reconstituted AAC show that caged nucleotides are competitive inhibitors (K_i = 5 μM for caged ADP and 1 μM for caged ATP). Caged ATP competes with photolyzed ATP as shown by the dependence of the currents on the caged ATP concentration and on the light intensity. A competition of added ADP with caged ATP on the currents yields K_i = 50 μM for ADP. We conclude that caged ADP and ATP bind tighter to AAC than ADP or ATP, allowing immediate initiation of translocation by in situ photolysis. The caged compounds bind preferentially at the cytosolic side of AAC. With a regenerative hexokinase+glucose system, the currents are stabilized in repetitive flashes and can be used for applying inhibitors etc. during a flash series. The currents are completely inhibited by the combined addition of the AAC inhibitors bongkrekate (BKA) and carboxyatractylate (CAT). The partial inhibition by CAT or BKA is dependent on the number of flash cycles increasing from 60% to 90%, and by replacing chloride with gluconate from only 30% to 90%. The currents are increased by a K^+ diffusion potential (valinomycin + KCl) and decreased by the permeant anion TPB^-. The pH dependence of the currents and of the parallel flux measurements indicates that only the fully charged ATP^{4-} and ADP^{3-} are transported. A strong temperature dependence of the currents with a break at 15 °C (E_A = 95 and 28 kJ) agrees with former measurements of flux rates in mitochondria. In conclusion, the capacitive currents faithfully reflect AAC transport function and are a powerful tool for investigating the charge transfer in transport.

The ADP/ATP transport in mitochondria is about the most active transport in eukaryotic cells and the terminal step of oxidative phosphorylation. First in mitochondria it was shown to be membrane potential dependent and thus to be electrically imbalanced (*1, 2*). With cation flux measurements, one positive charge was found to accompany the ATP/ADP exchange, and that one negative charge is involved in the ATP versus ADP exchange (*2, 3*). Since no Mg^{2+} is involved, it was concluded that ATP^{4-} exchanges against ATP^{3-} (*1*). Further, with the isolated and reconstituted ADP/ATP carrier (AAC),[1] the electrical imbalance of the heteroexchange modes ATP versus ADP and the elecroneutrality of the homoexchange modes were demonstrated (*4*). Here a proportionality between the ATP/ADP transport rates and the membrane potential was determined.

These findings required important alterations in the H^+ stoichiometry of ATP production outlined in the chemiosmotic theory, where an electroneutral ATP/ADP exchange was postulated (*5*). On balance, the ATP^{4-}/ADP^{3-} exchange withdraws about one-fourth of the H^+ pumped by the respiratory chain for the ATP delivered to the cytosol [see review (*6, 7*)]. As a result, the P/O ratio is decreased but the phosphorylation potential of the cytosolic ATP is elevated by about 3−4 kcal above that of the matrix ATP. Because of this fundamental importance of the electrical nature of the ADP/ATP exchange in bioenergetics, a further investigation of the details of this charge transfer is of great interest.

As reported in a previous paper (*8*), using AAC-reconstituted vesicles attached to a planar bilayer lipid membrane, we have applied a new method to measure the electrical fluxes involved in the ADP/ATP exchange by using an approach which was successfully employed to study ion pumps from the plasma membrane [for review, see (*9*)]. Capacitive currents generated by the AAC-catalyzed nucleotide transport could be measured after a rapid nucleotide concentration jump elicited by UV flash photolysis of caged nucleotides. Apart from the expected currents caused by the hetero-ADP versus ATP exchange, these first experiments

† This work was supported by a grant from the Deutsche Forschungsgemeinschaft (Kl 134/32-1).

* To whom correspondence should be addressed at the Institute of Physical Biochemistry, University of Munich, Schillerstrasse 44, D-80336 Munich, Germany. Telephone: +49-89-5996473. FAX: +49-89-5996415.

‡ University of Munich.

§ Max-Planck-Institute for Biophysics.

⊗ Abstract published in *Advance ACS Abstracts,* October 15, 1997.

[1] Abbreviations: AAC, ADP/ATP carrier; CAT, carboxyatractylate; BKA, bongkrekic acid; NEM, *N*-ethylmaleimide; TPP^+, tetraphenylphosphonium cation; Val, valinomycin; TPB^-, tetraphenylborate anion; $\Delta\psi$, electrical transmembrane potential; DTT, dithiothreitol.

S0006-2960(97)01578-X CCC: $14.00

brought some unexpected results. Even with AAC liposomes containing no ATP or ADP and in homoexchange systems, small currents were detected which were proposed to reflect partial reactions in the molecular cycle of the AAC (*8*).

To better understand the relation of the capacitive currents to ADP/ATP transport, we report here on the interaction of the caged nucleotides with the AAC. Further, the influence of basic parameters on capacitive currents is studied, such as pH, temperature, and transmembrane electrical potential ($\Delta\psi$). Also the influence of the specific inhibitors CAT and BKA, of extra- and intravesicular ADP, and of various SH reagents is investigated.

MATERIALS AND METHODS

Isolation and Reconstitution of AAC. The isolation and reconstitution of the AAC have been described previously (*8*). Briefly, mitochondria were solubilized with 3% Triton X-100. The AAC was enriched by hydroxyapatite chromatography in a batch procedure. The AAC-containing supernatant was added to solubilized egg yolk phospholipid and thoroughly dispersed. For loading of the vesicles with nucleotides, the desirable amounts of ADP or ATP were added to the mixture. The AAC-containing vesicles were generated by gradual removal of detergent with Amberlite XAD-2. For the removal of the external solutes, the AAC vesicle suspension was passed through a Sephadex G-75 column (30 × 1 cm).

Rat liver mitochondria were isolated by a conventional method of differential centrifugation from the livers of adult Wistar strain rats. Submitochondrial particles were prepared from bovine heart mitochondria as described by (*10*). Bovine heart mitochondria were prepared as described by Blair (*11*) and frozen in liquid nitrogen.

[^{14}C]ADP Flux Measurements. To check whether caged nucleotides can be transported by the AAC, we have measured the [^{14}C]ADP release from mitochondria which were preloaded with ^{14}C-labeled nucleotide as it was described in (*12*). To estimate the rate of [^{14}C]ADP release, we used the inhibitor-stop method (*13*). To study an interaction of the caged nucleotides with reconstituted AAC, the [^{14}C]ADP$_{ex}$−ADP$_{in}$ exchange in the presence of caged nucleotides was measured in ADP-loaded AAC vesicles (*14*).

Electrical Measurements. The electrical measurements were performed as described previously (*8*). Black lipid membranes with an area of 10^{-2} cm^2 were formed in a Teflon cell filled with appropriate electrolyte solution (1.5 mL for each compartment). The membrane-forming solution contained 1.5% (w/v) diphytanoyllecithin and 0.025% (w/v) octadecylamine in *n*-decane to obtain a positively charged membrane surface (*9*). Membrane formation was controlled by eye, and the capacitance of the membrane was determined. To photolyze the caged nucleotides, UV light pulses with an intensity of 2 W/cm^2 and 125 ms duration from a mercury high-pressure lamp (Zeiss, Oberkochen, Germany) were used. Quartz optics were employed throughout.

Reconstituted AAC liposomes were added to the rear compartment with respect to the light source in a medium containing 100 mM NaCl, 20 mM Hepes−Tris, pH 6.8, under gentle stirring. The experiment was started when the adsorption of the vesicles reached steady state (≈45−50 min after addition of the AAC vesicles). Caged ATP [*P*^{3}-1-(2-nitrophenyl)ethyl ester of ATP] was added under gentle stirring 10 min before the flash. A high buffer concentration was used to avoid fast protonation of the bilayer by the photolysis reaction of caged ATP which can also yield a transient current. The amplitudes of the currents within the same preparation of the vesicles varied no more than 20%. Control experiments with 100 μM c-ATP or c-ADP without vesicles or with phospholipid only gave a negligible signal (≤0/.2 nA/cm^2). The currents were measured with a Stanford Research System SR 570 amplifier and monitored on a Nicolet 310 storage oscilloscope.

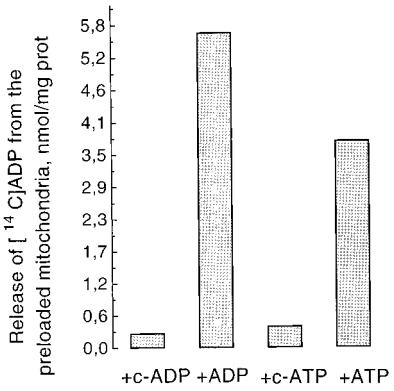

FIGURE 1: Caged ADP and caged ATP do not exchange with endogenous adenine nucleotides in rat liver mitochondria. The release of [^{14}C]adenine nucleotides from rat liver mitochondria was measured at 15 °C as described (*12*). Additions: all nucleotides in 100 μM concentration.

RESULTS

In the previous work on the electrical currents generated by AAC-linked transport, we have studied six different transport modes of the AAC: two heteroexchange modes (ATP/ADP and ADP/ATP), two homoexchange modes (ADP/ADP and ATP/ATP), and two unidirectional transport modes with unloaded AAC vesicles (ATP/− and ADP/−) (*8*). The main purpose of the present work is to investigate the influence of various factors on the AAC-generated currents in more detail and to understand the interaction of the caged nucleotides with the AAC. Therefore, we confined the experiments to only one transport mode, i.e., to the heteroexchange mode (ATP/ADP), by using external caged ATP with ADP-loaded vesicles.

Caged Nucleotides Are Not Transported by the AAC. The inability of the caged compounds to participate in enzymatic and transport reactions is the basic prerequisite to use these compounds in biochemical and biophysical studies. Since it was demonstrated in earlier papers that caged ATP can be bound to the transport ATPases (*15*), it was important to know whether the caged nucleotides can be bound to AAC without being transported. For these studies, we used rat liver mitochondria preloaded with [^{14}C]ADP. Addition of ADP or ATP to the mitochondria induced efflux of [^{14}C]-ADP in exchange with external nucleotides (Figure 1). However, caged ADP and caged ATP failed to induce a significant release of [^{14}C]ADP from the mitochondria. The small efflux of [^{14}C]ADP could be due to traces of free nucleotides in the caged nucleotide preparations. Thus, one can conclude that caged ADP and caged ATP are not transported by the AAC.

Electrical Currents Induced by the Rapid Jump of ATP Concentration. The flash-photolysis of caged ATP causes

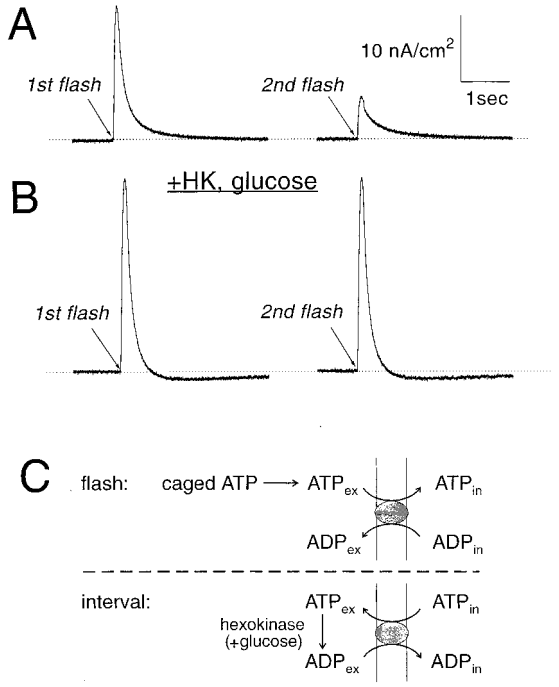

FIGURE 2: Recordings of the capacitive currents generated by the reconstituted AAC under UV flash photolysis of caged ATP in the absence (A) and in the presence (B) of hexokinase (HK) and glucose. The conditions of the experiments are described under Materials and Methods. The AAC vesicles were loaded with 10 mM ADP. For adsorption to the black membrane, AAC vesicles were incubated 50 min in the rear compartment of the chamber under gentle stirring before the first flash. All additions are on the same side of the black membrane under gentle stirring. Hexokinase (5 units) and glucose (1 mM) have been added 2−3 min before caged ATP. The flashes were applied 10 min after the addition of caged ATP (100 μM). Flash duration was 0.125 s. Temperature 23°C. (C) Mechanism of the regeneration of the ADP gradient on the liposomal membrane. For explanation, see the text.

a rapid concentration jump of free ATP (*16*). In the AAC-catalyzed reaction, the liberated ATP^{4-} is exchanged with intravesicular ADP^{3-} and thus induces an electrical current. Figure 2 shows typical current recordings obtained with the ADP-loaded AAC-reconstituted liposomes attached to the black membrane. The second flash induces a significantly reduced current, probably due to exhaustion of the ADP gradient (Figure 2A). To determine the influence of the internal ADP content on the currents, vesicles with various internal ADP concentrations were prepared (Figure 3). The current amplitudes increased strongly up to 10 mM ADP which must be taken to mean that the amount of internal ADP even at up to 10 mM was largely replaced by the exchange against the external photolyzed ATP. In agreement, the second flash produced a much lower current which was independent of the internal ADP loading. Obviously, the flash generates an excess of ATP to completely exhaust the internal ADP pool.

To study the influence of various factors on the electrical currents, an experimental system is required which is capable of generating constant repetitive signals. For this purpose, the internal ADP pool was regenerated after each flash by adding hexokinase+glucose. Thus, the excess of external ATP, liberated by the flash, is converted into ADP (see scheme in Figure 2C). During the 5 min intervals between the flashes, this external ADP largely replaces the intravesicular ATP taken up following the previous flash. As shown in Figure 2B, the addition of hexokinase+glucose

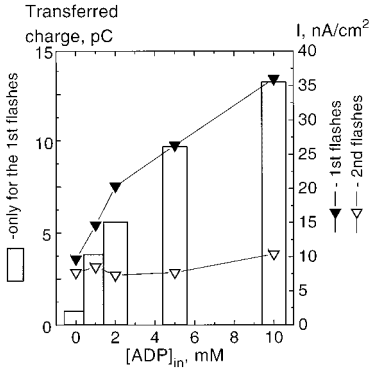

FIGURE 3: Dependence of the current amplitude and amount of charge transfer on the concentration of ADP in liposomes. Unloaded and AAC vesicles loaded with different concentrations of ADP were used. The concentration of caged ATP was 100 μM in all cases. The experiments were performed as described in the the legend to Figure 2. The second flash was 10 min after the first. Between the flashes, the solution in the chamber was under gentle stirring. The charge transferred was calculated (after base line subtraction) by numerically integrating from the start of the current to the point where the base line was reached again.

enables us to generate repetitive signals (up to 10−15) with nearly constant amplitude and identical shape. Interestingly, in the presence of hexokinase+glucose, a distinct negative overshoot appears, following the decay phase of the positive current. We propose that this overshoot reflects the reflux of net negative charge from the vesicles due to back-exchange, $ADP_{ex}-ATP_{in}$. As an additional benefit, hexokinase+glucose eliminates trace contamination of free ATP in the caged ATP preparation and thus protects against a partial discharge of the ADP gradient before the first flash. Thus, in the presence of hexokinase+glucose already the first flash induces a higher current than in their absence.

Interaction of Caged ATP with the Reconstituted AAC. According to the single-binding center-gated pore mechanism (equivalent to alternating-site or ping-pong mechanism) initially elucidated for the AAC, the binding site has a different conformation in the c- and m-states [see review (*7*)]. Therefore, the affinities of caged ADP and ATP for the sites in the two states should be different. To assess this case, the inhibition by caged ATP of the transport in mitochondria and in submitochondrial particles was assayed in which the AAC exposes either the "c" (cytosolic) or the "m" (matrix) side; 20 μM caged ATP inhibis the exchange (measured as [^{14}C]ADP efflux) in mitochondria to 61% and in submitochondrial particles (measured as [^{14}C]ATP uptake) only to 21%, after correction for the CAT- and BKA-insensitive efflux or uptake. The stronger effect of caged ATP from the c-side than from the m-side indicates that caged ATP has a preference to binding to the c-state of the AAC.

To understand the mechanism of current generation, it is important to know how tight caged ATP is bound to the AAC before the flash. Two different approaches were used to demonstrate an interaction of the caged nucleotides with the AAC. The first is based on following the effect of the competition between ATP and caged ATP on the current amplitude by varying the photolyzed ATP/caged ATP ratio or by varying the concentration of caged ATP at a constant rate of photolysis. This was achieved either by changing the caged ATP concentration or by increasing the flash intensity. This approach was formerly applied to demonstrate an interaction of caged ATP with Na^+/K^+-ATPase (*17*)

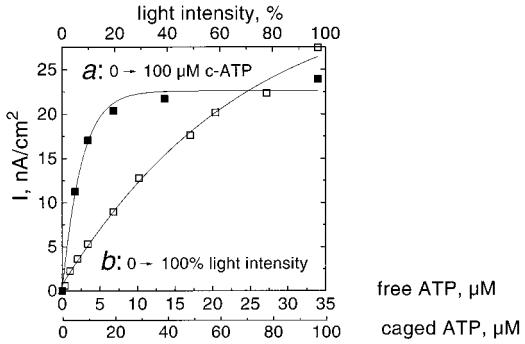

FIGURE 4: Dependence of the currents on the concentration of liberated ATP. Trace ***a***, the conversion rate was always 35%, and the ATP concentration was increased varied by sequential additions of caged ATP into ATP. Trace ***b***, the initial concentration of caged ATP was kept constant at 100 μM, and the ATP concentration was increased by stepwise increasing the flash intensity. The current measurements were performed in the presence of hexokinase+glucose as described in the legend to Figure 2.

(Figure 4). In experiment a, with constant light intensity, increasing concentrations of caged ATP produce a constant ratio (=0.35) of released ATP/caged ATP. In experiment b, at a given concentration of caged ATP, the increase of the flash intensity gives increasing ratios of released ATP/caged ATP from 0 to a maximum of 0.35. The current amplitudes plotted versus the calculated concentrations of the liberated ATP are clearly higher the greater the released ATP/caged ATP ratio as in experiment a. This indicates that caged ATP competes with free ATP for the AAC binding site. The slight flattening of the current versus high intensity might indicate an increased competition of ATP with caged ATP. Since this contrasts to the about 10-fold higher affinity of the caged ATP to the free nucleotides seen by transport measurements, another yet unexplained case may be involved.

Another line of more direct evidence for the competition between the caged nucleotides with the free nucleotides comes from measurements of the rate of [^{14}C]$ADP_{ex}-ADP_{in}$ exchange in AAC liposomes (Figure 5). These experiments were performed at 50 and 100 μM [^{14}C]ADP in the presence of increasing concentrations of caged ADP or caged ATP. The linearized plots $1/V_K$ versus [caged ADP] and [caged ATP] show a competitive type of inhibition by the caged nucleotides with $K_i = 1.5$ μM for caged ADP and $K_i = 5$ μM for caged ATP. Thus, the caged nucleotides bind to the AAC with higher affinity than free ADP or ATP (see Discussion). Caged GTP also inhibits [^{14}C]ADP_{ex}-ADP_{in} exchange although with lower efficiency ($K_i = 20$ μM) (not shown).

The competition between ADP and caged ATP for the AAC can also be visualized with the photolysis-induced currents (Figure 6) by adding external ADP. Using 10 and 100 μM caged ATP and increasing the concentration of ADP_{ex} from 2 to 200 μM, a clear competition between ADP_{ex} and caged ATP is seen. The apparent inhibition constant of the currents by ADP_{ex} is $K_i = 50$ μM. Thus, ADP_{ex} competes for the binding with caged ATP to the AAC only weakly with a K_i which is 10 times higher than that of caged ATP. These results also indicate that the concentrations of ADP, which are generated in the presence of hexokinase+glucose under repetitive flashes, are too low to significantly inhibit the currents.

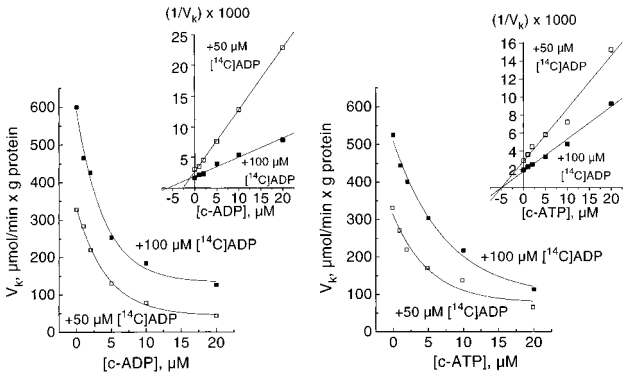

FIGURE 5: Caged nucleotides are competitive inhibitors of [^{14}C]-$ADP_{ex}-ADP_{in}$ exchange. V_k is the rate of [^{14}C]ADP−ADP exchange. Insets show the Dixon plots of the inhibition by caged ADP and caged ATP, respectively. The exchange reaction was initiated at 15 °C by addition of [^{14}C]ADP at concentrations of 50 or 100 μM to the AAC vesicles loaded with 20 mM ADP and stopped after 5, 10, 20, 40, and 300 s by addition of 10 μM CAT and 10 μM BKA. Each sample contained 150 μL of the vesicles. External nucleotides were removed from the vesicles by small Dowex 1-X8 anion exchange columns (2 × 0.4 cm), preequilibrated with 100 mM acetate, 0.5% BSA, and 1% phosphatidylcholine in order to minimize nonspecific adsorption. The samples were eluted with 100 mM acetate. The amount of [^{14}C]ADP taken up was measured in the eluted fractions. The increasing concentrations of caged ADP or caged ATP were added to the AAC vesicles 10 min before [^{14}C]ADP addition.

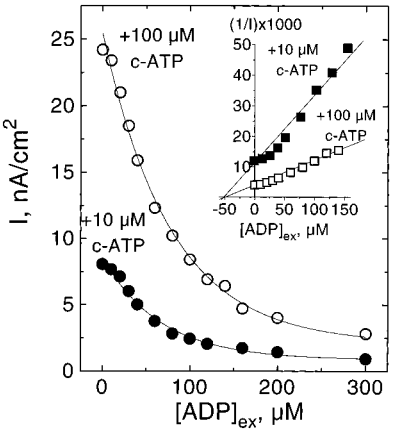

FIGURE 6: Dependence of the amplitude of the currents on the concentration of ADP_{ex}. The experiments were performed with two concentrations of caged ATP (c-ATP): 10 and 100 μM. The inset shows the inverse plot for the inhibition with $K_i = 50$ μM for ADP_{ex}.

Influence of Inhibitors of AAC. In our previous paper (*8*), we demonstrated that the specific inhibitors of the AAC, CAT and BKA added together, completely inhibit the currents. Thus, we can definitely attribute the currents to transport through the AAC. In addition, the AAC inhibitors allow us to determine the orientation of the carrier molecules responsible for the currents. CAT is impermeant and binds only to the cytosolic side of the AAC, whereas BKA can penetrate the membrane and bind to the matrix side of the carrier. The extent of CAT inhibition reflects the right-side-out orientation of the AAC and should be constant for the given preparation of the AAC liposomes.

CAT or BKA, added to the medium separately, decreased the amplitude of the current by up to 70% (Figure 7A). Further addition of the complementary inhibitor (BKA to CAT or CAT to BKA) completely blocked the currents. Surprisingly, we found that the efficiency of the inhibition

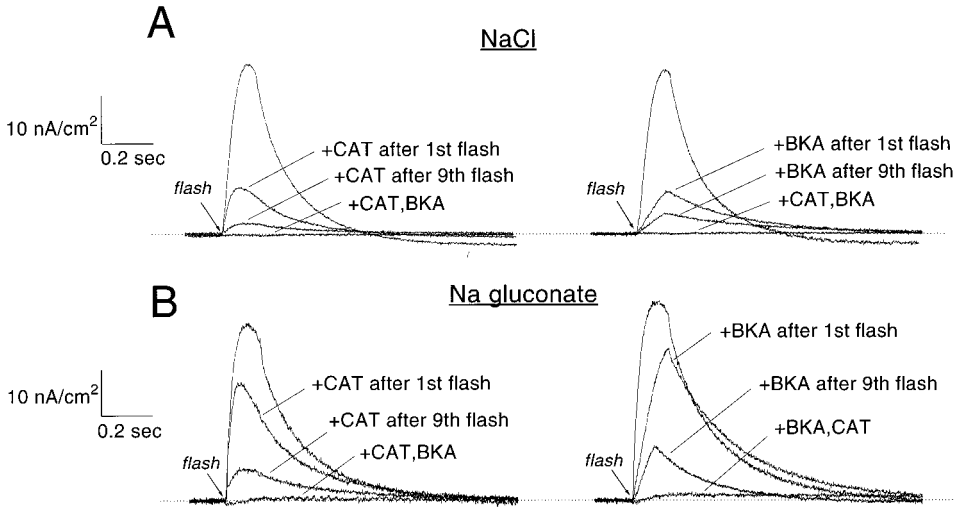

FIGURE 7: Effects of carboxyatractylate (CAT) and bongkrekic acid (BKA) on the currents and the influence of the number of flashes and of the anion species in the medium. Part A, the experiments were performed in 100 mM NaCl, 20 mM Hepes−Tris, pH 6.8 (NaCl medium); part B, the experiments were performed in 100 mM sodium gluconate, 20 mM Hepes−Tris, pH 6.8 (sodium gluconate medium). The inhibitors were added into the medium immediately after the first flash or after the ninth flash as indicated. The repetitive flashes were applied with a 10 min interval. Between flashes, the medium was stirred. Hexokinase (HK), 5 units, and glucose, 1 mM, were added in the medium 2−3 min before caged ATP.

depends on the number of the flashes performed before the inhibitors were added. If the inhibitors were added separately after 9−10 repetitive flashes, almost complete inhibition of the currents (up to 90−95%) was observed (Figure 7). To exclude accumulated ADP as the efficiency enhancer, in experiments not shown, the addition of ADP (5−10 μM) prior to UV irradiation of the AAC liposomes with caged ATP failed to simulate this effect. On the same line, repetitive flashes with caged ATP in the cuvette before addition of the AAC liposomes did not increase the inhibition. To exclude an UV-induced oxidation, DTT was added but could not prevent the repetitive flash increase of inhibition. Noteworthy, the efficiency of CAT and BKA depended also on the ionic composition of the medium. In a NaCl medium, the inhibition by CAT or BKA was significantly stronger than in sodium gluconate medium (Figure 7).

Effects of $\Delta\psi$, pH, and Temperature. The acceleration by the membrane potential of the ATP/ADP exchange in mitochondria and in the reconstituted system suggested its electrophoretic nature (*1, 4, 18*). Also the currents generated in the caged $ATP_{ex}-ADP_{in}$ system are increased by a K^+ diffusion potential generated by KCl plus valinomycin, which is positive inside of liposomes (Figure 8). Interestingly, in the presence of $\Delta\psi$, the negative overshoot vanished which was normally observed in the presence of hexokinase+glucose. The effect of the valinomycia-induced membrane potential is primarily to accelerate the ATP^{4-} versus ADP^{3-} exchanges. This charge movement is not compensated by a parallel K^+ movement because of the uphill potential gradient. In the reversed exchange, during the dark period, K^+ flux compensates the charges following the $\Delta\psi$ gradient. In agreement with this interpretation, addition of the lipophilic anion TPB^- decreases the currents. Here the counter movement of the largely membrane-bound TBP^- can compensate partially the charge translocation in the $ATP_{ex}-ADP_{in}$ exchange.

pH and Temperature Dependence. The pH dependence of the currents is of great interest in view of the possible involvements also of the protonated forms $ATPH^{3-}$ and

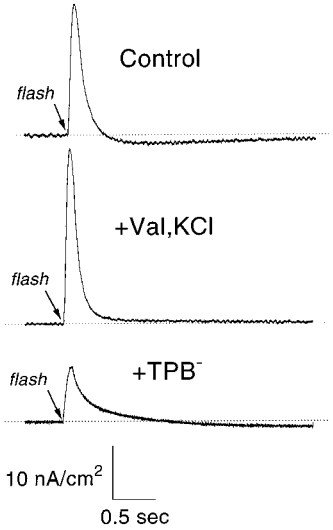

FIGURE 8: Influence of K^+ diffusion potential and of TPB^- on the currents. Currents from two separate experiments are shown. The experiments were performed as described in the legend to Figure 2. Before addition of valinomycin and KCl or TPB^-, two control flashes were performed. The amplitude and shape of the control signals were identical. In the experiment with valinomycin and KCl, the former (1 μM) was added 30 min before the flash under gentle stirring. KCl was added in 30 mM concentration into both compartments of the chamber 1 min before the flash under more intensive stirring. In another experiment, TPB^- (1 μM) was added after control flashes 30 min before the next flash.

$ADPH^{2-}$ in transport, which have a p$K \approx 6.7$ and thus can form a major share of the total ATP or ADP. An admixture of the $ATPH^{3-}/ADP^{3-}$ exchange mode to the ATP^{4-}/ADP^{3-} mode would give less than one charge per total ATP transported. We therefore compared the pH dependence of the currents with that of the exchange rates as measured in the vesicles.

As shown in Figure 9, the pH dependence of the capacitive currents has a similar pattern as the exchange rates. Since the rate of ATP liberation due to photolysis of caged nucleotide increases at lower pH (*16*), the pH optimum for the amplitude of the capacitive currents is slightly shifted to the lower pH values. Allowing for this influence, the pH

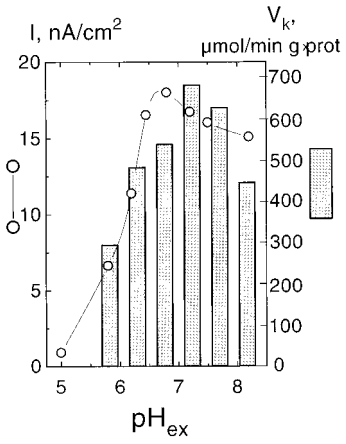

FIGURE 9: pH dependences of current amplitude and of [^{14}C]-$ADP_{ex}-ADP_{in}$ exchange with the reconstituted AAC. The capacitive currents were measured as described in the legend to Figure 2. [^{14}C]$ADP_{ex}-ADP_{in}$ exchange was measured as described in the legend to Figure 6.

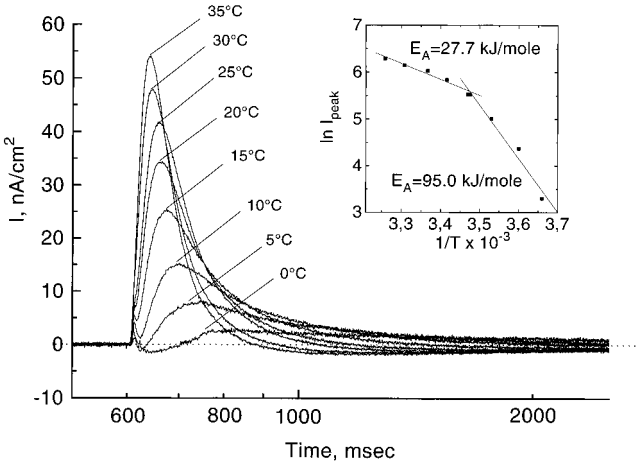

FIGURE 10: Temperature dependence of current amplitude. These currents were recorded with the same black membrane and attached AAC liposomes as described in the legend to Figure 2 at different temperature. The inset shows the Arrenius plot for the amplitudes of the capacitive currents.

dependencies of the capacitive currents and of the [^{14}C]-$ADP_{ex}-ADP_{in}$ exchange are in good agreement, indicating that the decrease of currents at low pH is due to the inability of the AAC to transport $ADPH^{2-}$.

The nucleotide exchange has been found to exhibit a strong temperature dependence (*19*). Correspondingly, the temperature should also influence the currents. Figure 10 shows the currents generated with caged ATP- and ADP-loaded AAC liposomes at different temperatures. There is a pronounced increase of the current amplitude with increasing temperature. The Arrhenius plot of the current amplitudes gives a break at about 15 °C. Below 15 °C, activation energies of $E_A = 92$ kJ and above 28 kJ are calculated. These data are in a good agreement with the temperature dependence of the flux measurements in mitochondria (*19*).

Effects of SH Reagents. The currents generated by flash-photolysis of caged ATP were also affected by SH reagents. Mersalyl (40 μM), added to the medium after several control flashes, significantly inhibited the currents (Figure 11A). Another hydrophilic SH reagent, 4-hydroxymercuribenzoate, had a similar effect (not shown). On the other hand, the more hydrophobic SH reagent NEM revealed pronounced inhibitory action only at the millimolar range (Figure 11B). The addition of the SH reductant DTT completely restored the currents inhibited by mersalyl but failed to restore the currents inhibited by NEM.

DISCUSSION

In the present work, an advanced technique is applied to the direct determination of electrical currents caused by the transport of ADP and ATP through AAC. With ADP-loaded AAC containing proteoliposomes attached to a black membrane, capacitive electrical currents were generated by initiating ATP/ADP exchange with a rapid photolytic ATP concentration jump. These results not only complement the former studies on the electrical nature of the ADP/ATP exchange (see the introduction), but also provide higher time resolution and eventually a more detailed insight into the substrate carrier interaction and the mechanism of nucleotide translocation. As shown in a preliminary publication (*8*), due to the high sensitivity and time resolution of this method, even partial steps in the reaction cycle of the AAC may be resolved. For example, with unloaded AAC liposomes, the method enabled us to detect currents which are supposed to occur in a half-turnover of the AAC.

After these first results, the following questions to characterize this system were asked. How do caged ADP and caged ATP interact with the AAC; i.e., do they bind to the AAC and are they transported? Is there a competition between the free and caged nucleotides? How do the inhibitors CAT and BKA affect the AAC-generated currents? What is the influence of pH, temperature, and $\Delta\psi$ on the currents?

As shown here with mitochondria, the caged nucleotides are not transported by the AAC. This is a prerequisite for their application to rapidly initiate transport on flash photolysis. There is a competition between the caged and the free forms for the AAC, as shown directly with the exchange in reconstituted vesicles.

The competitive inhibition constants ($K_i = 1$ and 5 μM for caged ATP and ADP) indicate that the caged forms bind considerably tighter to the AAC than the free forms. Former binding studies on mitochondria gave $K_D = 7$ μM for ADP and 12 μM for ATP (*20*), and after isolation and reconstitution, the affinity decreases further (unpublished results). In agreement, conversely ADP inhibits the caged ATP-induced currents with $K_i = 50$ μM. The comparatively tight binding of caged ADP and caged ATP can be very useful. Thus, the binding site is easily saturated with the caged compounds, and the bound caged nucleotides could release free nucleotides directly at the carrier binding site. Several substituted ADP or ATP derivatives are known to bind to the AAC with a considerable affinity. So far, most of these substitutions have been targeted to the 3′-position at the ribose (*21*−*23*) or to the 8- and 2-positions of the purine (*24*, *25*). Although the selectivity for the translocation by the AAC is extremely high and confined to ADP and ATP (*26*), there is more tolerance for the mere binding to the AAC. The tighter binding of a nontransportable ADP or ATP analogue, such as the caged ATP or ADP, is in line with the "induced transition fit" theory of carrier catalysis (*27*). According to this concept, the binding energy of a nontransportable ligand can be higher since its intrinsic binding energy is not partially compensated by the energy required for the induced transition fit of a transportable ligand.

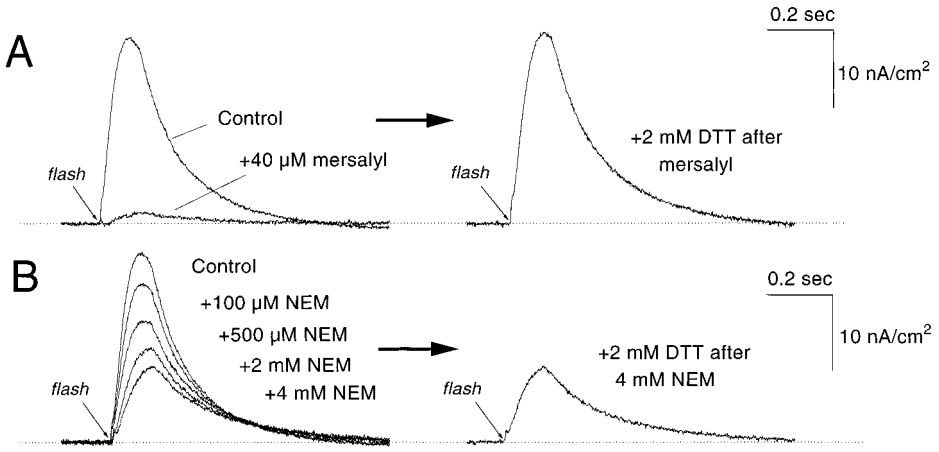

FIGURE 11: Effects of the SH reagents mersalyl (A) and *N*-ethylmaleimide (NEM) (B) on the currents. The experiments were performed as described in the legend to Figure 2. The SH reagents were added into the chamber under gentle stirring after two control flashes, 5 min before the next flash. The concentrations are indicated. DTT was added into the chamber after the flash with the SH reagents, 5 min before the subsequent flash. DTT added before the SH reagents did not influence the currents.

The about 2.5-fold decrease of the current amplitude on shifting the pH from 7.2 to 6.0 can have two reasons: (i) translocation of $ATPH^{3-}$ and $ADPH^{2-}$, which at pH 6.0 amounts to about 60% of the total concentration, is impeded and/or (ii) protonation of a critical amino acid of the AAC inhibits the exchange. The coincidence of the decrease of both the currents and the exchange rates argues for the first cause, the exclusion of $ATPH^{3-}$ and $ADPH^{2-}$. In fact, these results support the notion that the AAC exclusively uses the fully charged forms ATP^{4-} and ADP^{3-} for transport.

The temperature dependence of currents with the dramatic switch from the high activation energy of 92 kJ to only 28 kJ at 15 °C strongly resembles that of the exchange measured on bovine heart mitochondria. This again illustrated the faithful reflection in the currents of the transport but in another dimension. In the bovine heart mitochondria, E_A changed from 143 kJ to 63 kJ at 14 °C (*19*). In a detailed discussion of the pertinent evidence from related literature, we argued that a lipid phase transition was probably not responsible for the temperature break. Instead, the effect was seen to reside within AAC. It can be reasoned that in the temperature range up to 15 °C a large conformational change within AAC is rate limiting the overall rate, as reflected in the high activation energy. The 3.5 times lower activation energy above 15 °C points to rate limitation by a diffusional step of the substrate close to or within the AAC with low activation energy.

The inhibition by CAT and BKA indicates that the currents are entirely due to the AAC-catalyzed ADP/ATP exchange. However, added separately, CAT and BKA inhibit the currents only partially (Figure 7). The sidedness of interaction of the inhibitors with the AAC might be partially responsible for this incomplete inhibition. CAT interacts with the AAC only from the cytosolic side whereas BKA binds to the AAC from the matrix side. Since CAT cannot cross the membrane, the extent of the CAT inhibition can be used to estimate the orientation of the carrier in the membrane.

Surprisingly, increasing numbers of reaction cycles with each photolytic flash make the AAC more susceptible toward the inhibitors. The mechanism of the AAC sensibilization cannot be due to decreased affinity for the inhibitors since CAT and BKA are present at saturating concentrations. A mere sensibilization by ADP accumulation is improbable since addition of ADP does not increase the sensitivity of the AAC toward the inhibitors in a subsequent flash. Since the total concentration of caged ATP falls only about 10% after 10 flashes, a lower competition between caged ATP and inhibitors can also be ruled out. An influence of nitrophenol liberated from caged ATP is excluded by an experiment where the same amount of caged ATP was photolyzed (10 flashes) in the presence of hexokinase+glucose before the addition of the AAC liposomes. Since DTT failed to prevent the effect of repetitive flashes, one can also exclude that the oxidation of the SH groups of the AAC is involved in the sensibilization of the carrier to the inhibitors.

The strong influence of different anions, i.e., Cl^- versus gluconate anion, on the sensitivity of the AAC toward BKA and CAT is noteworthy (Figure 7). In the presence of sodium gluconate instead of NaCl as an osmolyte, the inhibition of the currents by CAT and BKA is much weaker, only 20−30% after the first flash, but can reach 70−80% after the ninth flash. It was noted earlier that various anions can inhibit nucleotide exchange by competition with ADP and ATP for the binding site (*28*). Thus, anions should also compete with caged ATP for binding to the AAC. Since Cl^- because of its smaller size is probably more effective than gluconate anion in penetrating and occupying the AAC binding site, binding of caged ATP to the AAC should be stronger in the presence of gluconate. Although CAT and also BKA are much stronger ligands for the AAC than nucleotides (*26*) they have to compete with the bound caged nucleotides. As a result, in the absence of Cl^-, the inhibitors may less efficiently compete with the caged ATP for the binding site. With this reasoning, the effect of the repetitive flashes on the efficiency of the inhibitors is due to an as yet unexplained decrease of the affinity of caged ATP after repetitive flashes.

SH reagents, such as mecurials and NEM, strongly inhibit the currents (Figure 11), in accordance with the well-characterized inhibition of ADP/ATP exchange in the flux measurements (*29*−*31*). Out of the four cysteines in bovine heart AAC (*32*), the preferred binding of NEM to C56 (*33*) and of the more polar eosin-5-maleimide to C159 (*34*, *35*) was determined. The surrounding positive charges were suggested to facilitate the interaction of the negatively

charged eosin-5-maleimide with C159. Also mersalyl, negatively charged as well, was proposed to interact with C159 like eosin-5-maleimide (*14*). The inhibition of the capacitive currents with SH reagents does not necessarily mean that the SH groups are important for the nucleotide transport. The mutation C73S in yeast AAC, at the homologue to the bovine heart C56, retains near-wild-type nucleotide transport activity (*36*). It was concluded that although cysteines are not essential for transport, the bound SH reagents block the translocating pathway near these cysteines.

In conclusion, the results presented in this paper demonstrate that the AAC is highly suitable for applying capacitive current measurements combined with caged ATP and ADP photolysis. Ideally, the caged compounds bind tightly to the carrier site without being transported. The currents generated by the AAC proved to be sensitive to various factors (pH, temperature, $\Delta\psi$, SH reagents, AAC inhibitors) in the same manner as determined for the nucleotide exchange by tracer measurements. This justifies the conclusion that the current measurements with their inherent high sensitivity and time resolution provide a powerful approach to study details of the AAC-catalyzed nucleotide transport.

ACKNOWLEDGMENT

We thank Gabriele Basset for her help in preparing the proteoliposomes and Anja Becker for help with the current experiments.

REFERENCES

1. Pfaff, E., and Klingenberg, M. (1968) *Eur. J. Biochem. 6*, 66−79.
2. Wulf, R., Kaltstein, A., and Klingenberg, M. (1978) *Eur. J. Biochem. 82*, 585−592.
3. LaNoue, K., Mizani, S. M., and Klingenberg, M. (1978) *J. Biol. Chem. 253*, 191−198.
4. Krämer, R., and Klingenberg, M. (1982) *Biochemistry 21*, 1082−1089.
5. Mitchell, P. (1979) *Eur. J. Biochem. 95*, 1−20.
6. Klingenberg, M. (1970) in *Essays in Biochemistry* (Campbell, P. N., and Dickens, F., Eds.) Vol. 6, pp 119−159, Academic Press, London/New York.
7. Klingenberg, M. (1976) in *The Enzymes of Biological Membranes: Membrane Transport* (Martonosi, A. N., Ed.) Vol. 3, pp 383−438, Plenum Publishing Corp., New York/London.
8. Brustovetsky, N., Becker, A., Klingenberg, M., and Bamberg, E. (1996) *Proc. Natl. Acad. Sci. U.S.A. 93*, 664−668.
9. Bamberg, E., Butt, H. J., Eisenrauch, A., and Fendler, K. (1993) *Q. Rev. Biophys. 26*, 1−25.
10. Klingenberg, M. (1977) *Eur. J. Biochem. 76*, 553−565.
11. Blair, P. V. (1967) *Methods Enzymol. 10*, 78−81.
12. Pfaff, E., Klingenberg, M., and Heldt, H. W. (1965) *Biochim. Biophys. Acta 104*, 312−315.
13. Gawaz, M. P., Douglas, M. G., and Klingenberg, M. (1990) *J. Biol. Chem. 265*, 14202−14208.
14. Brustovetsky, N., and Klingenberg, M. (1994) *J. Biol. Chem. 269*, 27329−27336.
15. Fendler, K., Jaruschewski, S., Hobbs, A., Albers, W., and Froehlich, J. P. (1993) *J. Gen. Physiol. 102*, 631−666.
16. McCray, J. A., Herbette, L., Kihara, T., and Trentham, D. R. (1980) *Proc. Natl. Acad. Sci. U.S.A. 77*, 7237−7241.
17. Nagel, G., Fendler, K., Grell, E., and Bamberg, E. (1987) *Biochim. Biophys. Acta 901*, 239−249.
18. Krämer, R., and Klingenberg, M. (1980) *Biochemistry 19*, 556−560.
19. Klingenberg, M., Grebe, K., and Appel, M. (1982) *Eur. J. Biochem. 126*, 263−269.
20. Weidemann, M. J., Erdelt, H., and Klingenberg, M. (1970) *Eur. J. Biochem. 16*, 313−335.
21. Mayer, I., Dahms, A. S., Riezler, W., and Klingenberg, M. (1984) *Biochemistry 23*, 2436−2442.
22. Block, M. R., Lauquin, G. J. M., and Vignais, P. V. (1982) *Biochemistry 21*, 5451−5457.
23. Block, M. R., and Vignais, P. V. (1984) *Biochim. Biophs. Acta 767*, 369−376.
24. Dalbon, O., Boulay, F., and Vignais, P. V. (1985) *FEBS Lett. 180*, 212−218.
25. Mayinger, P., Winkler, E., and Klingenberg, M. (1989) *FEBS Lett. 244*, 421−426.
26. Klingenberg, M. (1985) in *The Enzymes of Biological Membranes* (Martonosi, A. N., Ed.) pp 511−553, Plenum Publishing Corp., New York.
27. Klingenberg, M. (1991) in *A Study of Enzymes, Vol. II: Mechanism of Enzyme Action* (Kuby, S. A., Ed.) pp 367−388, CRC Press, Boca Raton/Ann Arbor/Boston.
28. Krämer, R., and Kürzinger, G. (1984) *Biochim. Biophys. Acta 765*, 353−362.
29. Leblanc, P., and Clauser, H. (1972) *FEBS Lett. 23*, 107−113.
30. Vignais, P. V., and Vignais, P. M. (1972) *FEBS Lett. 26*, 27−31.
31. Aquila, H., and Klingenberg, M. (1982) *Eur. J. Biochem. 122*, 141−145.
32. Aquila, H., Misra, D., Eulitz, M., and Klingenberg, M. (1982) *Hoppe-Seyler's Z. Physiol. Chem. 363*, 345−349.
33. Boulay, F., and Vignais, P. V. (1984) *Biochemistry. 23*, 4807−4812.
34. Majima, E., Koike, H., Hong, Y. M., Shinohara, Y., and Terada, H. (1993) *J. Biol. Chem. 268*, 22181−22187.
35. Majima, E., Shinohara, Y., Yamaguchi, N., Hong, Y. M., and Terada, H. (1994) *Biochemistry 33*, 9530−9536.
36. Hoffmann, B., Stöckl, A., Schlame, M., Beyer, K., and Klingenberg, M. (1993) *J. Biol. Chem. 269*, 1940−1944.

BI971578X